ACS APPLIED BIO MATERIALS

Article

Cite This: ACS Appl. Bio Mater. 2019, 2, 3212−3224

www.acsabm.org

Mechanistic Study on the Antibacterial Activity of Self-Assembled Poly(aryl ether)-Based Amphiphilic Dendrimers

Ramya Kannan,[†,‡] Palani Prabakaran,[†] Ruchira Basu,[†] Chinmai Pindi,[‡] Sanjib Senapati,[‡] Vignesh Muthuvijayan,[*,‡] and Edamana Prasad[*,†]

[†]Department of Chemistry, Indian Institute of Technology Madras (IIT M), Chennai 600036, India

[‡]Department of Biotechnology, Bhupat And Jyoti Mehta School of Biosciences, Indian Institute of Technology Madras (IIT M), Chennai 600036, India

Supporting Information

ABSTRACT: The increased threat of bacterial resistance against conventional antibiotics has warranted the need for development of membrane targeting antibacterial agents. Several self-assembled cationic amphiphiles with different supramolecular structures have been reported in recent years for potent antibacterial activity with increased specificity. In this study, we describe the self-assembly and antibacterial activity of four lower generation poly(aryl ether)-based amphiphilic dendrimers (**AD-1**, **AD-2**, **AD-3**, and **AD-4**) containing terminal amine (PAMAM-based), ester, and hydrazide functional groups with varied hydrophobicity. Among the four dendrimers under study, the amine-terminated dendrimer (**AD-1**) displayed potent antibacterial activity. The ratio of surface cationic charge to hydrophobicity had a significant effect on the antibacterial activity, where **AD-3** dendrimer with increased surface cationic charges exhibited a higher minimum inhibitory concentration (MIC) than **AD-1**. **AD-2** (ester terminated) and **AD-4** (hydrazide terminated) dendrimers did not show any bactericidal activity. The amphiphilic dendrimer−bacteria interactions, further validated by binding studies, also showed significant changes in bacterial morphology, effective membrane permeation, and depolarization by **AD-1** in comparison with **AD-3**. Molecular dynamics simulations of **AD-1** and **AD-3** on bacterial membrane patches further corroborated the experimental findings. The structural conformation of **AD-1** dendrimer facilitated increased membrane interaction compared to **AD-3** dendrimer. **AD-1** also displayed selectivity to bacterial membranes over fibroblast cells (4× MIC), corroborating the significance of an optimal hydrophobicity for potent antibacterial activity with no cytotoxicity. The self-assembled (poly(aryl ether)-PAMAM-based) dendrimer (**AD-1**) also exhibited potent antibacterial activity in comparison with conventional higher generation dendrimers, establishing the implication of self-assembly for bactericidal activity. Moreover, the detailed mechanistic study reveals that optimal tuning of the hydrophobicity of amphiphilic dendrimers plays a crucial role in membrane disruption of bacteria. We believe that this study will provide valuable insights into the design strategies of amphiphilic dendrimers as antibacterial agents for efficient membrane disruption.

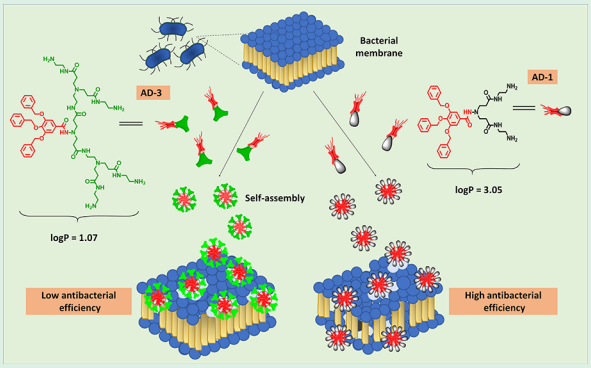

KEYWORDS: *amphiphilic dendrimer, self-assembly, antibacterial activity, membrane disruption, hydrophobicity, poly(aryl ether) dendron, PAMAM*

INTRODUCTION

Bacterial infection is regarded as one of the never-ending issues related to the health of humans, and the recent emergence of antibiotic-resistant microorganisms has become a great threat to society.[1−3] The alarming increase in the resistance of bacteria against antibiotics has led to worldwide research on new antimicrobial molecules.[4−6] Bacterial cell wall and certain intracellular biochemical processes (DNA or protein synthesis) are the most sought-after targets for antibiotics to date. However, resistance against conventional antibiotics has brought in the need for other less conserved bacterial targets.[7,8] Bacterial membranes, on the other hand, have a conserved structure whose delayed prospectus of resistance development is an advantage for designing membrane-targeted antibiotics. Moreover, the permeability of antibacterial compounds will not be of primary concern, unlike antibiotics targeted toward the intracellular biochemical process.[9,10] Nonetheless, the close similarity of the eukaryotic and prokaryotic cell membrane is a key concern for the usage of bacterial membranes as targets for antibiotics. However, some fundamental differences exist between the eukaryotic and prokaryotic cell membranes.

Received: February 18, 2019
Accepted: May 24, 2019
Published: May 24, 2019

DOI: 10.1021/acsabm.9b00140
ACS Appl. Bio Mater. 2019, 2, 3212−3224

Hence, a rationale in the design of molecules for specifically targeting bacterial membranes is the need of the hour.[11]

Antimicrobial peptides (AMPs) are a class of membrane targeting molecules with a broad spectrum of antibacterial activity, extensively studied as a substitute for antibiotics. AMPs are known for their amphiphilic nature and cationic surface charges. Cationic surface charge is known to facilitate strong electrostatic interaction with the bacterial membrane, and the hydrophobic moiety disrupts the membrane by integration to the lipophilic interior.[12,13] Regardless of the biocompatibility and potent antibacterial activity of AMPs, proteolytic degradation and short half-lives deter clinical translations of antimicrobial peptides.[14] Hence, as an alternate to AMPs, synthetic peptide mimics,[15,16] cationic surfactants/small molecules,[17−19] and polymers/peptide conjugates are currently being investigated.[20−22]

Recently, the innate activity of AMPs has been attributed to the self-assembly and aggregation of the amphiphilic structure.[23] Self-assembly, a well-known phenomenon for the formation of different supramolecular structures, has been widely used for various biomedical applications.[24,25] Also, self-assembled cationic amphiphilic peptides with well-defined structures such as micelles or nanorods have exhibited potent antibacterial activity due to their high surface charge and increased local mass.[26−31] While different antibacterial polymers with various supramolecular structures have also displayed enhanced antibacterial activity,[32,33] the polydispersity of polymers and tedious synthesis of peptides have facilitated research on amphiphilic cationic small molecules.

Peptide-based dendrimers,[34] polyamidoamine (PAMAM)[35] and polyethylenimine (PEI) dendrimers[36] have been studied for their antibacterial activity. Though the antibacterial activity of higher generation PAMAM-based dendrimers with different chemical functionalities has already been reported,[37,38] the tiresome synthetic procedures of higher generation dendrimers and their cytotoxicity leading to nonspecific membrane disruption are major limitations. On the other hand, poly(aryl ether)-based dendrons, known for their branched multifunctional periphery with a high propensity to self-assemble,[39−43] have not been explored for their antibacterial activity. Specifically, a novel combination of poly(aryl ether) dendron-PAMAM-based amphiphilic dendrimer was recently reported by our group, which displayed solvent-dependent self-assembly and gelation.[44] However, the intrinsic antibacterial activity of poly(aryl ether)-PAMAM-based amphiphilic dendrimers has not been investigated so far, to the best of our knowledge. Furthermore, the correlation between such supramolecular structures and the antimicrobial activity is less explored. More importantly, there still exists a need for developing a design approach for tuning the cationic charge, hydrophobicity, and self-assembly of cationic amphiphiles for potent antibacterial activity.

Therefore, we intend to explore the mechanistic aspects of poly(aryl ether)-PAMAM-based amphiphilic dendrimers for potential antibacterial activity. In this work, four poly(aryl ether)-based amphiphilic dendrimers with different terminal spacers containing amines, ester, and hydrazide units were successfully constructed and observed for their antibacterial activity and mechanism of action. Preliminary spectroscopy and morphology studies elucidated the structural characteristics and self-assembly nature, followed by the antibacterial activity of the amphiphilic dendrimers on Gram-positive and Gram-negative bacteria. Our main aim is to comprehend the structural attributes of the amphiphilic dendrimers to facilitate a potent antibacterial activity with high specificity. Fluorescence-based membrane disruption and depolarization assays were performed to understand the mechanism of bacterial membrane disruption by the amphiphilic dendrimers. Molecular dynamics simulations were also performed to elucidate the significance of the structural attributes of the dendrimers for membrane interaction. In addition, cytotoxicity of the amphiphilic dendrimers was tested on mouse fibroblast cells to verify the membrane specificity to prokaryotes. The results discussed herein provide useful strategies to design amphiphilic molecules with a tunable hydrophobicity and cationic charge for effective self-assembly and enhanced bactericidal activity.

EXPERIMENTAL SECTION

Materials and Instruments. All the chemicals obtained from commercial sources were of analytical purity and used without further purification unless mentioned. All NMR spectra were recorded in Bruker 500 MHz spectrometer Avance series (^{1}H:400 MHz; ^{13}C:100 MHz) at a constant temperature of 298 K with tetramethylsilane $SiMe_4$ (TMS) used as the internal reference for the ^{1}H and ^{13}C NMR analysis. Mass spectra for the compounds were recorded using a Micromass Q-TOF mass spectrometer. UV−vis spectra were recorded in a JascoV-660 spectrophotometer using a 1 cm quartz cuvette. Surface morphologies were captured by a scanning electron microscope (SEM) HITACHI S 4800 instrument. The aggregate samples were prepared by drop-casting the samples onto indium tin oxide (ITO) plates followed by vacuum drying at room temperature and were subjected to gold sputter coating for 90 s using a HITACHI E-1010 ion sputter. Dynamic light scattering (DLS) analysis and zeta potential measurements were conducted on Malvern instrument Zetasizer nano ZS90. Ninety-six-well plate MTT assay absorbance was measured using a Bio-Rad X mark microplate reader. Fluorescence assay measurements were recorded using a PerkinElmer Enspire multimode plate reader.

General Synthetic Procedure of the Amphiphilic Dendrimers. Amphiphilic dendrimers **AD-1** and **AD-2** of a poly(aryl ether) dendron linked with PAMAM-based dendrimer were synthesized based on a previously reported procedure.[44] In addition to this, a higher generation of PAMAM terminated dendrimer (**AD-3**) and a hydrazide terminated dendrimer were synthesized (**AD-4**). The detailed synthetic procedure and their structural characterization is given in the Supporting Information (Figures S1−S6)

Structural Characteristics of the Amphiphilic Dendrimers. Theoretical lipophilicity measurements were calculated using a virtual computational chemistry laboratory (VCC lab) with ALOGPS 2.1 software.[45] The SMILE strings of compounds **AD-1**, **AD-2**, **AD-3**, and **AD-4** were submitted, and the logP values were predicted by ALOGPS 2.1. The pK_a of the four amphiphilic dendrimers were predicted by Marvin sketch (18.30.0).

Self-Assembly Studies. The self-assembly of the amphiphilic dendrimers were monitored by UV−vis spectroscopy, and the formed aggregates were visualized by SEM technique. The size of the aggregates was further confirmed by DLS, and zeta potential was also measured.

Bacterial Culture Conditions. *Staphylococcus aureus* (ATCC 25923) (*S. aureus*), a Gram-positive bacterial strain, and *Escherichia coli* (ATCC 25922) (*E. coli*), a Gram-negative bacterial strain, were used as model microorganisms for our study. Luria−Bertani (LB) broth was used as the medium for our bacterial assays unless specified otherwise. Both the bacterial strains were thawed from frozen stocks and subcultured prior to their use in experiments. The overnight grown cultures were freshly inoculated in LB broth and maintained at 37 °C, 180 rpm to reach the mid log phase (OD600 = 0.5) for all bacterial inhibition assays.

Stock Solutions of Amphiphilic Dendrimers for Bacterial Studies. **AD-1**, **AD-2**, and **AD-4** dendrimers of 5 mg/mL each were prepared in DMSO as a stock, and the solutions were reconstituted in LB broth at specific concentrations for the experiments. **AD-3** was

DOI: 10.1021/acsabm.9b00140
ACS Appl. Bio Mater. 2019, 2, 3212−3224

dissolved in miliQ water or LB broth directly as per the experimental conditions.

Minimum Inhibitory Concentration (MIC). The bactericidal activity of the amphiphilic dendrimers was evaluated by the broth microdilution method.[46] As previously stated, overnight grown *E. coli* and *S. aureus* cultures were diluted in fresh LB broth and grown at 37 °C until mid log phase. The four amphiphilic dendrimers were serially diluted in the LB broth in a 96-well microtiter plate to a final volume of 100 μL. Bacterial inoculum making up to 5×10^6 CFU/well was further added to the 96-well plates. Three controls, namely, wells containing bacterial suspension, bacterial suspension with kanamycin antibiotic, and last bacterial suspension with DMSO diluted as per the experimental conditions, were maintained. After 24 h of incubation at 37 °C, the plates were visually observed for turbidity and change in optical density (OD) using a multiplate reader at 600 nm. The lowest compound concentration that yields no visible growth is generally recorded as the MIC.

Minimum Bactericidal Concentration (MBC). To determine the MBC, MIC samples from the well plates were serially diluted in LB media and plated on LB agar. Colonies were counted after overnight incubation at 37 °C, and the colony forming units (CFUs)/mL was calculated. MBC is defined as the lowest concentration of an antibacterial agent required to kill the bacteria where there is no colony observed on the plate.

Time-Kill Studies. Overnight grown bacterial cultures of *E. coli* and *S. aureus* were subcultured into fresh 50 mL LB broth in a conical flask and maintained at 37 °C to reach mid log phase (0.6 OD). The amphiphilic dendrimers **AD-1**, **AD-2**, **AD-3**, and **AD-4** (250 μg/mL) were added separately to the inoculum. The mixtures were incubated at 37 °C at 150 rpm. Bacterial cultures with no treatment were maintained as control. Sample aliquots from the suspensions were taken at 0, 3, 6, 12, and 24 h, and the OD was measured. The aliquots were serially diluted, and 10 μL of culture was plated on an LB agar plate. The plates were then incubated at 37 °C for 24 h, and the bacterial colonies were counted and quantified by colony forming unit per mL.

Zeta Potential Studies. Zeta potential values were measured using Zetasizer Nano ZS (Malvern Instruments). The amphiphilic dendrimers were serially diluted from 2 mg/mL to 0.015 mg/mL in HEPES buffer, pH 7.4. To these samples, a bacterial inoculum of a mid log phase culture was inoculated. Bacterial cultures with no treatment were maintained as the control. The samples were equilibrated for 15 min and transferred to a glass cuvette with a zeta electrode for measurement. The zeta potential values were recorded and plotted against the concentration of the amphiphilic dendrimers.

Esterase Activity by (cFDA-SE) Assay. Carboxyfluorescein diacetate-succinimidyl ester (cFDA-SE) is a bacterial cell wall and membrane permeable dye which is nonfluorescent and becomes fluorescent upon being hydrolyzed by esterase enzymes. The esterase activity of live bacteria is monitored by the change in fluorescence of the dye, which correlates to membrane disruption.[47] A stock solution of cFDA-SE (500 μM) was prepared in ethanol and used. Overnight grown *S. aureus* and *E. coli* cells were centrifuged at 8000 rpm for 5 min, washed with PBS, and resuspended to achieve a cell concentration of 10^6 CFU/mL. To this, 50 μM of cFDA-SE as a final concentration was added and incubated for 20 min at 37 °C. The cells were then centrifuged, washed twice with sterile PBS to remove excess cFDA-SE molecules, resuspended in 1.0 mL of sterile PBS, and treated with **AD-1**, **AD-2**, **AD-3**, and **AD-4** (250 and 500 μg/mL each) at 37 °C and 180 rpm for 2 h. In the case of the control sample, only DMSO was added to the cFDA-SE labeled cells and incubated under the same conditions. Fluorescence measurements were performed for determining the leakage of cFDA from cells from the supernatant samples at an excitation wavelength of 488 nm by collecting the emission at 518 nm.

Propidium Iodide (PI) Binding Assay. Propidium iodide is a nucleotide staining dye, which is cell wall impermeable. PI stains membrane-damaged cells, not staining the membrane-intact cells.[47] A stock solution of PI (1.5 mM) prepared in sterile Milli-Q water was used for monitoring membrane impairment. Overnight grown *S. aureus* and *E. coli* cells were centrifuged, washed and resuspended in sterile PBS. Cells (approximately 10^6 CFU/mL) were treated with the amphiphilic dendrimers (250 and 500 μg/mL each) and incubated at 37 °C, 180 rpm for 2 h. Cells incubated in DMSO under the same conditions without amphiphile were included as the control. Post incubation, the cells were washed with sterile PBS twice and incubated with 30 μM of PI as the final concentration for 30 min at 37 °C. The cells were then centrifuged, washed with sterile PBS to remove supernatants and the pellet was resuspended in PBS. The fluorescence of PI was measured at 617 nm with an excitation wavelength of 535 nm.

Microscopy Analysis. Overnight grown cells of *S. aureus* and *E. coli* were centrifuged and resuspended in PBS. Approximately 10^6 CFU/mL cells were treated with **AD-1** and **AD-3** at their respective MICs for 2 h at 37 °C. Control samples consisted of untreated cells incubated in PBS for the same period. After the treatment time, the bacterial cells were centrifuged at 8000 rpm for 5 min and washed twice with PBS. The cells were fixed in 2.5% glutaraldehyde for 2 h at 4 °C, centrifuged, washed and resuspended in sterile miliQ water. A 10 μL aliquot of each sample was spotted on ITO plates and air-dried in a laminar hood, followed by ethanol dehydration procedures. The samples were dehydrated in an ethanol series (50, 70, and 90%) for 5 min each and 100% ethanol for 15 min. The air-dried samples were gold sputtered for 90 s using HITACHI E-1010 ion sputter and imaged by the scanning electron microscope HITACHI S 4800 instrument.

Membrane Depolarization Assay. 3,3′-Dipropylthiadicarbocyanine iodide ($DiSC_3 5$) is a cationic membrane potential sensitive dye that is known to accumulate on hyperpolarized membranes, displaying decreased fluorescence upon integration to the bacterial membrane.[48] To study the depolarization of bacterial membrane by our compounds **AD-1** and **AD-3**, $DiSC_3 5$ was used. *S. aureus* and *E. coli* cells in the mid log phase were collected by centrifugation and washed and resuspended in HEPES buffer (5 mM HEPES, 20 mM glucose, pH 7.4). $DiSC_3 5$ (0.4 μM) was added to the cell suspension and kept for 1 h at 37 °C, after which 100 mM of KCl was added and incubated for 15 min. The bacterial mixtures and the control were monitored for a change in fluorescence over time for 10 min. The fluorescence emission at 670 nm was measured with an excitation at 622 nm.

Molecular Dynamics Simulations. To understand the structural attributes of **AD-1** and **AD-3** on bacterial membrane interactions, we performed molecular dynamics simulations of bacterial membrane patches with both the dendrimers. The fully hydrated membrane patches of roughly 100 × 100 Å with the composition of 126 POPE (1-palmitoyl-2-oleoyl-*sn*-glycero-3-phosphoethanolamine) and 42 POPG (1-palmitoyl-2-oleoyl-*sn*-glycero-3- phospho-(1′-rac-glycerol) with a ratio of (3POPE:1POPG) molecules in both the leaflets were obtained from the CHARMM-GUI web portal.[49] These membranes were minimized and equilibrated based on previous reports.[50] Subsequently, molecular dynamics (MD) simulations were performed for membrane alone for 10 ns. The geometries of **AD-1** and **AD-3** were optimized by Hatree-Fock 6-31G (d,p) method using Gaussian09 package.[51] Further, the parameters of the dendrimers were obtained using antechamber from the AMBER package.[52] The membrane−dendrimer complexes were built by placing the individual molecule at the center of the membrane surface in such a way that the distance between any atom of the dendrimer from the surface was at least 8 Å, and there was no initial penetration of any atom into the membrane. Detailed information on the molecular dynamics simulation steps and the energy calculations are given in the Supporting Information (Page S-13)

Cell Culture. NIH/3T3 cell lines of mouse fibroblast origin were purchased from the National Center for Cell Science (Pune, India) and were cultured. The NIH/3T3 cells were maintained in Dulbecco's modified Eagle's medium (DMEM, Himedia) supplemented with 10% fetal bovine serum (Invitrogen), penicillin (100 μg/mL), and streptomycin (100 μg/mL) in a 5% CO_2 incubator.

Cell Cytotoxicity Assay. To test the biocompatibility of **AD-1**, **AD-2**, **AD-3**, and **AD-4**, dimethylthiazol-2-yl)-2,5-diphenyltetrazolium bromide (MTT) assay was performed based on a previously reported procedure.[53] Eighty percent confluent cells were trypsinized and seeded on to a 96-well plate (1×10^4 cells/well), and the plates were incubated for 24 h for attachment. Stock solutions of **AD-1**, **AD-2**, and **AD-4** were prepared with cell culture grade DMSO and diluted to concentrations

DOI: 10.1021/acsabm.9b00140
ACS Appl. Bio Mater. 2019, 2, 3212−3224

Scheme 1. Synthetic Scheme of the Amphiphilic Dendrimers AD-1, AD-2, AD-3, and AD-4

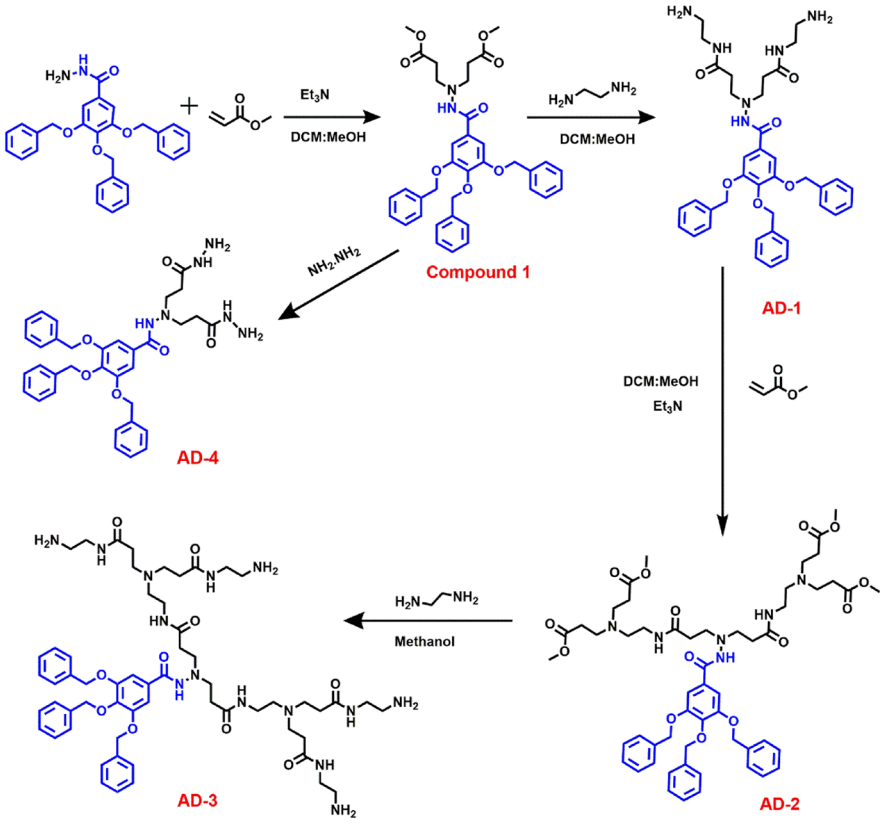

ranging from 2−0.0312 mg/mL in DMEM. **AD-3** was dissolved in DMEM media at the same concentrations. The cells were treated with the dendrimers and incubated for 24 and 48 h. The incubated cells were then washed with PBS and tested for their cytotoxicity by MTT assay. MTT dye was added, and the plates were kept in the dark for 4 h. After the formation of formazan crystal, DMSO was added, and the absorbance was measured at 570 nm with 670 nm as the reference. Each experiment was done in triplicate. Mean and standard deviation (SD) were tabulated and plotted. The cell viability was calculated based on the equation:

$$\%\ \text{cell viability} = \left(\frac{\text{mean OD}}{\text{control OD}}\right) \times 100$$

Statistical Analysis. Two-way ANOVA with post-test of Bonferroni was performed for all the *in vitro* experiments using GraphPad Prism (version 5.0) software. The values $^{*}p < 0.05$, $^{**}p < 0.01$, and $^{***}p < 0.001$ were considered statistically significant.

RESULTS AND DISCUSSION

The cationic surface charge of polyamidoamine dendrimers (PAMAM) and the hydrophobicity of peptide amphiphiles are known for their potent bactericidal activity.[34,54] Intrinsic antibacterial property of PAMAM dendrimers and their generation-dependent cytotoxicity have also been investigated.[5,55] Along with hydrophobicity and surface charge, self-assembly of peptide amphiphiles has been exploited recently for its effective bacterial membrane disruption. The self-assembly and aggregation propensity of amphiphiles are reported to have an advantage over the monomeric peptides/small molecules.[50,56] We previously reported the self-assembly and gelation of two novel Janus dendrimers containing poly(aryl ether) dendron-PAMAM dendrimer in different solvents and solvent mixtures. The synergistic effect of $\pi-\pi$ stacking and H-bonding led to the formation of a highly robust three-dimensional network.[44] However, their intrinsic bactericidal activity was not explored. Hence, in the present study, we hypothesize that the influence of amphiphilicity and the surface charge of the poly(aryl ether) dendron-PAMAM based dendrimers (**AD-1** and **AD-2**) could be effective against bacterial membranes. Moreover, to investigate the structural characteristics of the amphiphilic dendrimers for potent antibacterial activity, higher generation PAMAM linked poly(aryl ether)-based amphiphilic dendrimer (**AD-3**) was synthesized. Also, to understand the protonation of terminal amines with different pK_a at the physiological pH, poly(aryl ether) dendron terminated with hydrazide units (**AD-4**) was synthesized.

AD-1 and **AD-2** were synthesized by amidation and esterification with excess ethylenediamine and methyl acrylate by our previously reported procedure.[44] While amidation of **AD-2** with ethylene diamine yielded **AD-3**, **AD-4** was synthesized by the reaction of compound 1 (dimethyl 3,3′-(2-(3,4,5-tris-(benzyloxy)benzoyl) hydrazine-1,1-diyl) dipropionate) with hydrazine hydrate. Scheme 1 depicts the synthetic steps involved in the preparation of **AD-1** to **AD-4**, and the detailed spectral data are given in the Supporting Information (Figures S1−S6).

Self-Assembly and Gelation. The gelation ability of **AD-1** and **AD-2** in specific solvent mixtures was previously reported.[44] The self-assembly, $\pi-\pi$ interaction, and H-bonding of the amphiphilic dendrimers (**AD-1** and **AD-2**) in different solvent mixtures were investigated, and the results exhibited a solvent-dependent morphology. In this study, the gelation abilities of **AD-3** and **AD-4** were tested in different solvents and solvent mixtures. It was observed that **AD-3** did not form gels in any of the solvents tested, while **AD-4** formed a stable gel in specific solvent mixtures. **AD-3** was found to be soluble in most polar

DOI: 10.1021/acsabm.9b00140
ACS Appl. Bio Mater. 2019, 2, 3212−3224

solvents and water, owing to the presence of increased terminal amines facilitating H-bonding with the solvent. The critical gel concentration (CGC) values of the amphiphiles are summarized in Table S1.

To monitor self-assembly, UV−vis studies for the amphiphilic dendrimers in DMSO:water mixture below their CGC were performed. The absorption maxima of **AD-1**, **AD-2**, and **AD-3** were found to be at 268 nm, while the absorption maximum of **AD-4** was observed at 280 nm. The absorption studies were carried out in DMSO, and the absorption peaks are assigned to $\pi-\pi$ transitions.[42] Upon addition of water, we found a gradual shift in the absorption maximum. The absorption band displayed a pronounced shift as the water fraction increased from 80 to 90%, exhibiting a blueshift in all four compounds (Figure 1). **AD-1** displayed a blueshift of 15 nm, while **AD-2** and **AD-3** displayed a 6−10 nm shift (Figure 1a−c). **AD-4** showed a shift of 18 nm (Figure 1d). The aggregation observed by UV−vis spectroscopy is indicative of H-aggregates, demonstrating the role of $\pi-\pi$ interactions in the self-organization process.

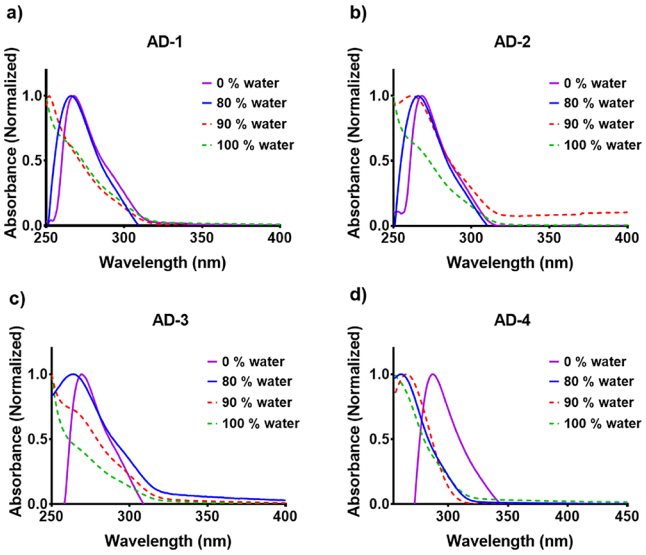

Figure 1. UV−vis spectra of 50 μM (a) **AD-1**, (b) **AD-2**, (c) **AD-3**, and (d) **AD-4** in DMSO with increasing water percent; the dotted line depicts the aggregation of the compounds in DMSO:water mixture.

Next, the morphology and size of the aggregates were investigated in DMSO:water (1:9 v/v) using SEM and DLS measurements (Figure 2a−h). The SEM images exhibited spherical aggregates for all the amphiphilic dendrimers (Figure 2a−d). The hydrodynamic size of the spherical aggregates varied between 200 and 300 nm for the amphiphilic dendrimers. The smallest among them was for **AD-2** dendrimer (201 ± 15 nm) with a polydispersity index (PDI) of 0.21 (Figure 2f). The amine-terminated dendrimers **AD-1** and **AD-3** were found to be 225 and 236 nm with the PDI of 0.81 and 0.93, respectively (Figures 2e and 2g). The hydrazide terminated **AD-4** dendrimer formed spherical aggregates of 267 nm with the PDI of 0.33 (Figure 2h and Table 1). The stability of the dendrimer aggregates (200 μg/mL) in PBS was monitored for 72 h. **AD-1**, **AD-2**, and **AD-3** dendrimers displayed minimal aggregation, while **AD-4** formed large visible aggregates over a longer period. The **AD-1**, **AD-2**, and **AD-3** aggregates exhibited only minimal size change up to 24 h, demonstrating the aggregate stability (Figure S7). Moreover, the stability of the amphiphilic dendrimers in biological media was also studied. Amphiphilic dendrimers **AD-1** to **AD-4** were monitored for their change in aggregate size in cell culture media (DMEM with 15% FBS) over 72 h. In cell culture media, the dendrimers **AD-1** to **AD-4** showed aggregation behavior similar to that in the buffer conditions, indicating no specific protein interactions (Figure S8).

Table 1. Physicochemical Properties of the Amphiphilic Dendrimers

	hydrodynamic size (d. nm)	logP value	zeta potential (mV)
AD-1	225 ± 20	3.05	9.38 ± 2.56
AD-2	201 ± 15	4.29	−8.5 ± 1.21
AD-3	236 ± 24	1.07	4.74 ± 1.45
AD-4	267 ± 55	3.99	−3.4 ± 2.23

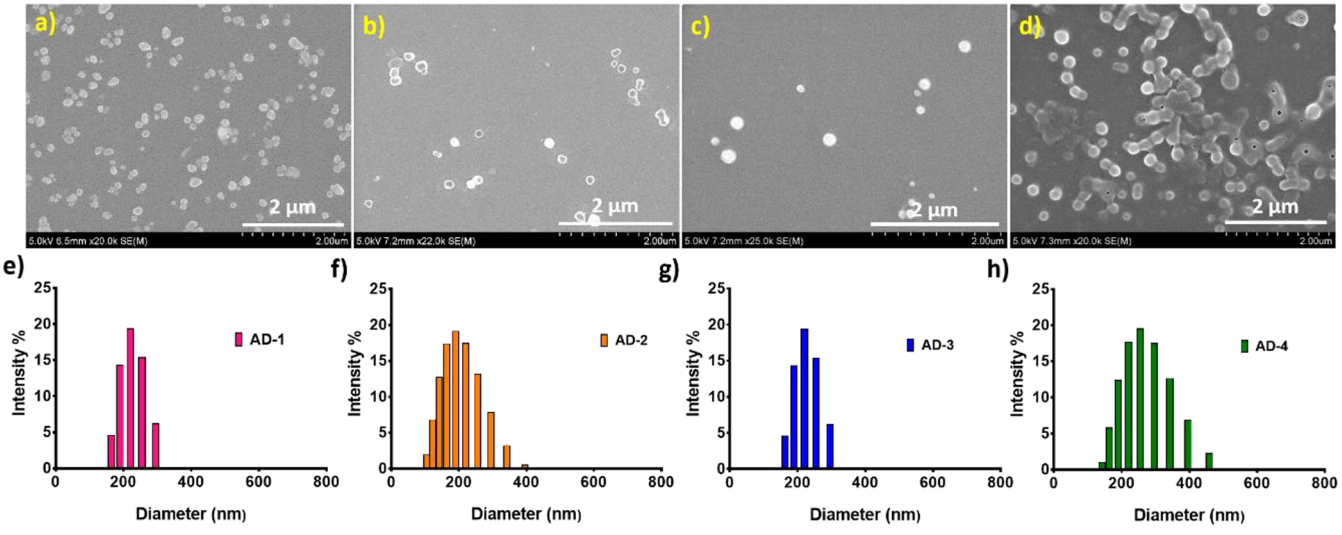

Figure 2. SEM images of the spherical aggregates of (a) **AD-1**, (b) **AD-2**, (c) **AD-3** (100% water), and (d) **AD-4** in DMSO:water (1:9 v/v); (e−h) DLS data of **AD-1**, **AD-2**, **AD-3**, and **AD-4**, respectively

DOI: 10.1021/acsabm.9b00140
ACS Appl. Bio Mater. 2019, 2, 3212−3224

Zeta potential measurements for all the amphiphilic dendrimers were measured in DMSO:HEPES buffer (1:9 v/v, pH 7.4), which indicated a positive zeta potential value of 9.38 ± 2.56 and 4.74 ± 1.45 mV for **AD-1** and **AD-3**, respectively. As anticipated, the ester terminated **AD-2** dendrimer showed a negative surface potential value of −8.5 ± 1.21 mV. On the other hand, the hydrazide terminated **AD-4** dendrimer also displayed a negative surface potential value of −3.4 ± 2.23 mV at the physiological pH (Table 1). This may be attributed to the difference in the protonation of amines and hydrazides in the physiological pH. To further validate this, the pK_a of amines and hydrazides was predicted at the physiological pH.

Structural Characteristics. To understand and elucidate the structural features of the designed molecules, theoretical predictions of the lipophilicity and pK_a of **AD-1**, **AD-2**, **AD-3**, and **AD-4** at pH 7.4 were calculated by AlogPs and Marvin sketch (18.3.0) software, respectively. From the zeta potential measurements, we understand that the protonation of the amphiphilic dendrimers is dependent on the pK_a of the terminal amines and hydrazides. To validate further, pK_a of our amphiphilic dendrimers were predicted by Marvin sketch (18.3.0), the results of which are presented in the Supporting Information (Figures S9−S16). The pK_a values of the primary (8.86−9.46), secondary (13.90), and tertiary amines (1.68) of **AD-1** were theoretically predicted (Figure S9). The distribution of the protonated form of **AD-1** at the physiological pH indicated that the primary amines were protonated at pH 7.4 (Figure S10). As expected, the ester terminated **AD-2** dendrimer remains unchanged at the physiological pH, as evidenced by the zeta potential value (Figures S11 and S12). **AD-3** with a higher generation of terminal amines also followed a similar trend in pK_a for the primary, secondary, and tertiary amines (Figure S13−S14). On the other hand, the pK_a of hydrazide terminated amphiphilic dendrimer (**AD-4**) was found to be 2.98−3.58 (Figure S15). Moreover, the distribution profile of **AD-4** also indicated that the microspecies found at the physiological pH are not protonated owing to its low pK_a (Figure S16). This further confirms the negative zeta potential of the compound at pH 7.4.

LogP is the partition coefficient of the molecule between water (aqueous phase) and octanol (oil phase). LogP is also regarded as the measure of the hydrophobicity of the compound and is recently being correlated for membrane integration and permeability.[57] Also, a study by Tomita et al. has shown the relationship between the hydrophilic−lipophilic balance (HLB) and antimicrobial activity. It has been reported that an optimal hydrophobicity is required to cause effective bacterial killing with no cytotoxicity.[58] Theoretical predictions of the amphiphilic dendrimers were calculated using the SMILE strings of the chemical structure. We found that there was a decrease in logP value with an increase in terminal amines. The logP of **AD-3** was found to be lower (1.07) in comparison with that of **AD-1** (3.05) due to the increase in amine functional groups, resulting in a more water-soluble hydrophilic molecule. On the other hand, ester and hydrazide terminated dendrimers **AD-2** and **AD-4** displayed higher logP values (Table 1).

The pKa and the logP values elucidated the structural differences in surface charge and hydrophobicity of the designed amphiphilic dendrimers. Based on these results, we hypothesized that the structural attributes of the designed amphiphiles (**AD-1** to **AD-4**) may play a significant role in bacterial membrane disruption.

Bacterial Inhibitions. The antibacterial activity of the amphiphilic dendrimers against *E. coli* and *S. aureus* were determined by a slightly modified broth microdilution method.[46] The amine-terminated dendrimers were anticipated to be effective against the bacterial strains due to their structural attributes of both cationic surface charge and hydrophobicity. The MIC of the dendrimers against both the bacterial strains was tabulated (Table 2). As expected, the MIC of the amine-terminated **AD-1** was found to be lower than those of the ester (**AD-2**) and hydrazide terminated (**AD-4**) dendrimers. However, to our surprise, **AD-3** dendrimer having a higher generation of terminal amine groups displayed MIC value higher than that of **AD-1**. This is probably due to the differences in the hydrophobicity of the amphiphilic dendrimers **AD-1** and **AD-3**. By the structural characteristics, we know that the pK_a values of both dendrimers (**AD-1** and **AD-3**) remain to be almost similar at the physiological pH. However, the logP values clearly demonstrate the differences in hydrophobicity among the two dendrimers **AD-1** and **AD-3**, which we correlate to the decrease in the MIC. The other two amphiphilic dendrimers **AD-2** and **AD-4** were found to be inactive against both the Gram-negative and Gram-positive strains at concentrations up to 2 mg/mL (Table 2). The MBC values for dendrimers **AD-1** and **AD-3** were also calculated and are presented in Table 2. The MIC results thus indicate that an amphiphile with higher hydrophobicity is more effective against bacteria. Previous reports on the spatial positioning of the hydrophobic groups of cationic amphiphiles have displayed potent antibacterial activity with minimal cytotoxicity.[59] Therefore, to understand the structural characteristics of the amphiphilic dendrimers for antibacterial activity, mechanistic studies were performed further.

Table 2. Antibacterial Activity of Amphiphilic Dendrimers Determined by the Broth Microdilution Method

	MIC (mg/mL)		MBC (mg/mL)	
	E. coli	*S. aureus*	*E. coli*	*S. aureus*
AD-1	0.062	0.031	0.125	0.031
AD-2	>2	2	>2	>2
AD-3	2	0.5	2	1
AD-4	>2	2	>2	>2

Time-Kill and Surface Charge Neutralization Assay. Time-kill studies on both *E. coli* and *S. aureus* were performed on liquid broth cultures. The colonies were counted to measure the bacterial reduction by treatment with amphiphilic dendrimers (250 μg/mL). **AD-1** showed the highest reduction in the bacterial growth on both microorganisms, followed by **AD-3**. The other two dendrimers **AD-2** and **AD-4** displayed minimal reduction on the bacterial count, indicating ineffective bacterial killing as evidenced by the MIC (Figures 3a and b). To further understand the neutralization of the bacterial membrane charge, change in zeta potential was investigated. Bacterial cells in 1:9 (DMSO: HEPES buffer, pH 7.4) was kept as control. In the absence of the dendrimer solutions, *E. coli* and *S. aureus* exhibited a zeta potential of −20 mV (Figure 3c) and −12 mV, respectively (Figure 3d). To the bacterial culture, amphiphilic dendrimer solutions at doubling dilutions were added, and the zeta potential was measured. The results clearly depict a decline in the zeta potential values of the control bacteria in the presence of the amphiphilic dendrimers (Figures 3c and d). Surprisingly, the decline in the zeta potential of the bacteria in the presence of both **AD-1** and **AD-3** was almost similar, which we attribute to

DOI: 10.1021/acsabm.9b00140
ACS Appl. Bio Mater. 2019, 2, 3212−3224

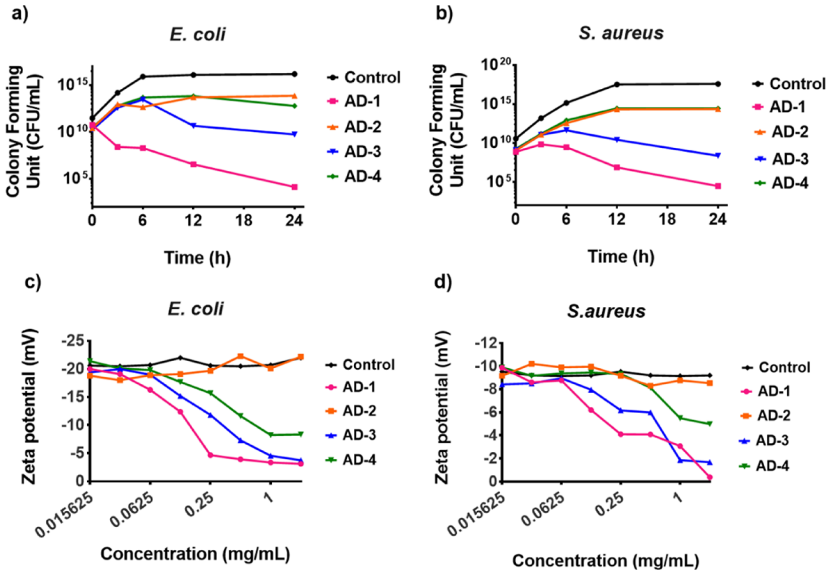

Figure 3. Time-kill assay of (a) *E. coli* and (b) *S. aureus* upon treatment with 250 μg/mL of amphiphilic dendrimers; (c and d) the effect of amphiphilic dendrimers on the zeta potential of *E. coli* and *S. aureus*, respectively.

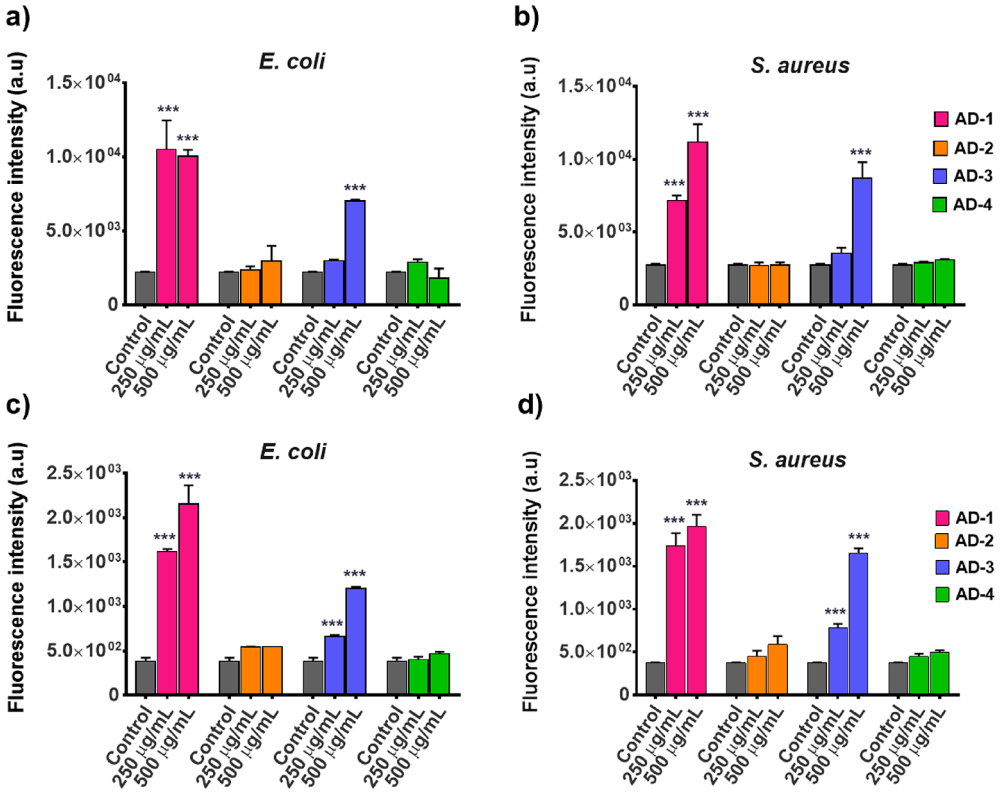

Figure 4. cFDA-SE leakage assay on target bacterial cells (a) *E. coli* and (b) *S. aureus* treated with amphiphilic dendrimers (250 and 500 μg/mL); propidium iodide assay on (c) *E. coli* and (d) *S. aureus* treated with amphiphilic dendrimers. Statistical analysis was calculated with respect to the control bacterial cells, $n = 3$, $^{**}p < 0.01$ and $^{***}p < 0.001$ vs control.

the role of the surface zeta potential of the aggregates and its protonation at physiological pH. Moreover, a steady decrease in the zeta potential of *E. coli* and *S. aureus* in the presence of **AD-4** was also observed, while the presence of **AD-2** did not show any change in the zeta potential of bacteria (Figures 3c and d). The observed differences for each amphiphilic dendrimer can be justified by the structural characteristics of the dendrimer. Most commonly, amphiphilic molecules are known to interact primarily with bacterial membranes by electrostatic interaction, resulting in the outer membrane permeation.[60] From the zeta potential changes observed in bacterial cells, we understand that both **AD-1** and **AD-3** display strong electrostatic interactions with the outer bacterial membrane but vary in their bactericidal activity. To further understand the mechanism of bacterial killing by the amphiphilic dendrimers, fluorescent assays to validate membrane disruption and depolarization were carried out.

DOI: 10.1021/acsabm.9b00140
ACS Appl. Bio Mater. 2019, 2, 3212−3224

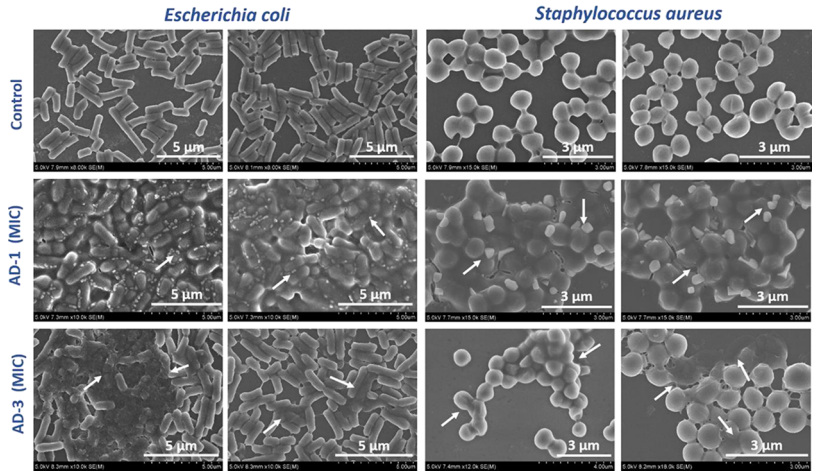

Figure 5. SEM images of *E. coli* and *S. aureus* before and after 2 h incubation with amphiphilic dendrimers **AD-1** and **AD-3** at their MIC concentration. (First row) Control bacterial cells of *E. coli* and *S. aureus*; (second row) **AD-1** dendrimer showing nanosized aggregates surrounding the bacterial cells; (third row) **AD-3** dendrimer treated cells displaying fused bacterial membranes.

Mechanism of Action of Amphiphilic Dendrimers. To validate the hypothesis of membrane targeting antibacterial activity, membrane disruption by the amphiphilic dendrimers was assessed by well-established fluorescent assays.[61] The cFDA-SE leakage assay monitors the intracellular esterase activity based on a fluorescent dye. Two concentrations (250 and 500 μg/mL) of the amphiphilic dendrimers were assessed for their activity, and it was found that the increase in fluorescence intensity was highly pronounced for **AD-1**. Control bacterial cells show minimal fluorescence, indicating an intact membrane, while the **AD-1** and **AD-3** treated bacteria show a dose-dependent increase in fluorescence for both *E. coli* and *S. aureus* (Figures 4a and b). Similarly, propidium iodide (PI) uptake assay is another fluorescence-based method to assess bacterial membrane damage. PI is a membrane-permeable dye which does not stain live bacteria. Upon treatment of the bacterial strains with amphiphilic dendrimers, we found that **AD-1** treated bacteria showed an increased fluorescence intensity compared to that of the control. **AD-3** also displayed a significant change in the fluorescence for both *E. coli* and *S. aureus* (Figures 4c and d). The membrane disruption studies correlate with the MIC and membrane neutralization studies. As expected, the two dendrimers **AD-2** and **AD-4** failed to display any change in fluorescence in both cFDA-SE and PI assays, indicating no antibacterial activity due to their surface charge.

From these results, we understand that **AD-1** dendrimer, bearing both the cationic surface functional moieties and an optimum hydrophobicity, displays potent antibacterial activity among the other amphiphilic dendrimers. It is further confirmed that **AD-3** dendrimer with higher amine moieties showed a reduction in the zeta potential of the bacteria upon treatment (Figures 3c and d), indicating strong electrostatic interactions with the bacterial membrane, but failed to show potent antibacterial activity. We attribute this to the long flexible spacer arm of **AD-3** dendrimer, which minimizes the lipid membrane interaction due to its hydrophilicity. On the other hand, short hydrophobic **AD-1** dendrimer is forced to insert into the lipid backbone, leading to effective antibacterial activity.[62] These results clearly demonstrate the need for both an optimal cationic charge and hydrophobicity of the amphiphiles to act as effective antibacterial agents. To further validate the membrane targeting activity of the amphiphilic dendrimers, bacterial morphology changes and membrane depolarization assays were performed with **AD-1** and **AD-3** dendrimers.

Bacterial Morphological Changes. SEM was used to visualize the changes in the morphology of bacterial cells upon treatment with the amphiphilic dendrimers **AD-1** and **AD-3** (Figure 5). The SEM images of the control groups display distinct rod and cocci shaped bacteria of *E. coli* and *S. aureus* with smooth walls (Figure 5, first row). The bacterial cells were about 2−3 μm in size. Upon treatment with **AD-1** and **AD-3** for 2 h at their respective MICs, the bacterial cells were merged and displayed change in morphology (Figure 5, second and third row). The SEM images of both *E. coli* and *S. aureus* cells treated with 0.125 mg/mL of **AD-1** displayed small sized aggregates of 200−300 nm surrounding the bacterial cell wall (Figure 5, second row). We attribute them to the self-assembled spherical aggregates of **AD-1** ranging around 250 nm, as evidenced by DLS and SEM (Figure 2). **AD-3** (2 mg/mL) treated bacterial cells were fused and were irregular in shape, encompassed by a matrix layer (Figure 5, third row). SEM images of **AD-1** treated bacteria after 12 h were also taken, which displayed disintegrated bacteria with changes in morphology (Figure S17).

On the basis of these evidences, we hypothesize that the amphiphilic dendrimers primarily surround the bacterial cell membrane, leading to electrostatic interactions between the cationic surface charge and the negative membrane potential. Then, the amphiphilic dendrimers disrupt the cell membrane, which results in the leakage of cytoplasm contents, leading to cell death.

Membrane Depolarization Assay. Membrane depolarization assay was performed by 3,3′-dipropylthiadicarbocyanine iodide ($DiSC_3S$), a membrane potential dye that accumulates in the bacterial membrane of energized cells giving no fluorescence. Upon treatment with the antibacterial molecules, the fluorescence intensity of the dye is enhanced, indicating membrane depolarization. The change in fluorescence of *E. coli* and *S. aureus* cells treated with 0.5 mg/mL of **AD-1** and **AD-3** was monitored over time. The change in fluorescence intensity of *E.coli* upon **AD-3** treatment was much lower than the fluorescence intensity of **AD-1** treated bacteria , as shown in Figure 6a. This is probably due to the high MIC value of 2 mg/mL for **AD-3** on *E. coli*. However, **AD-3** treated *S. aureus* cells displayed a similar enhancement in the fluorescence intensity as

DOI: 10.1021/acsabm.9b00140
ACS Appl. Bio Mater. 2019, 2, 3212−3224

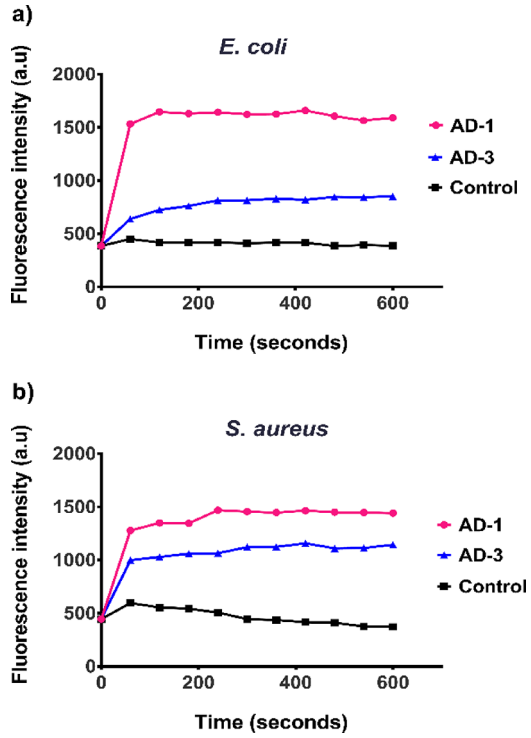

Figure 6. $DiSC_3$5-based membrane depolarization assay kinetics of (a) *E. coli* and (b) *S. aureus* cells treated with 0.5 mg/mL of amphiphilic dendrimers **AD-1** and **AD-3**

compared to **AD-1** treated bacteria, as evidenced by their MIC (Figure 6b). The membrane depolarization results corroborate the time-kill studies and MIC of the amphiphilic dendrimers, suggesting the significance of hydrophobicity of the molecules for effective antibacterial activity.

From these results, we state that the initial electrostatic interactions help in decreasing the surface potential of bacteria, causing membrane depolarization, but the hydrophobicity determines the potency of bacterial killing. Moreover, the differences in fluorescence intensity enhancement of *E. coli* and *S. aureus* cells treated with **AD-3** dendrimers depicted the strong electrostatic interaction between Gram-positive organism in comparison to Gram-negative microbes. Similar to amphiphilic peptides, the results herein revealed the antibacterial activity of poly(aryl ether)-based amphiphilic dendrimers by membrane disruption. All four amphiphilic dendrimers self-assembled to form stable spherical nanosized aggregates. The hydrophobicity of **AD-1** and **AD-3** dendrimers varied due to the presence of a flexible extended amine dendrimer, which makes **AD-3** more hydrophilic than **AD-1**. The optmimal balance of cationic surface charge and hydrophobicity of the amphiphilic dendrimers (**AD-1** and **AD-3**) showed a correlation with antibacterial activity. The increase in hydrophobicity clearly demonstrated an increased affinity for membrane permeation and bacterial death, as reported previously.[28,63]

Structural Attributes of Dendrimers AD-1 and AD-3 on Membrane Interactions. Although experimental evidences indicated the significance of nanostructured aggregates of **AD-1** and **AD-3** dendrimers on bacterial membrane disruption, MD simulations with single molecule entities were performed to elucidate the structural attributes of the designed dendrimers on membrane interactions. Previous reports on the MD simulations of cationic amphiphiles with variable hydrophobicity revealed that along with surface charge and hydrophobicity, conformational reorientation of the amphiphiles is more likely to

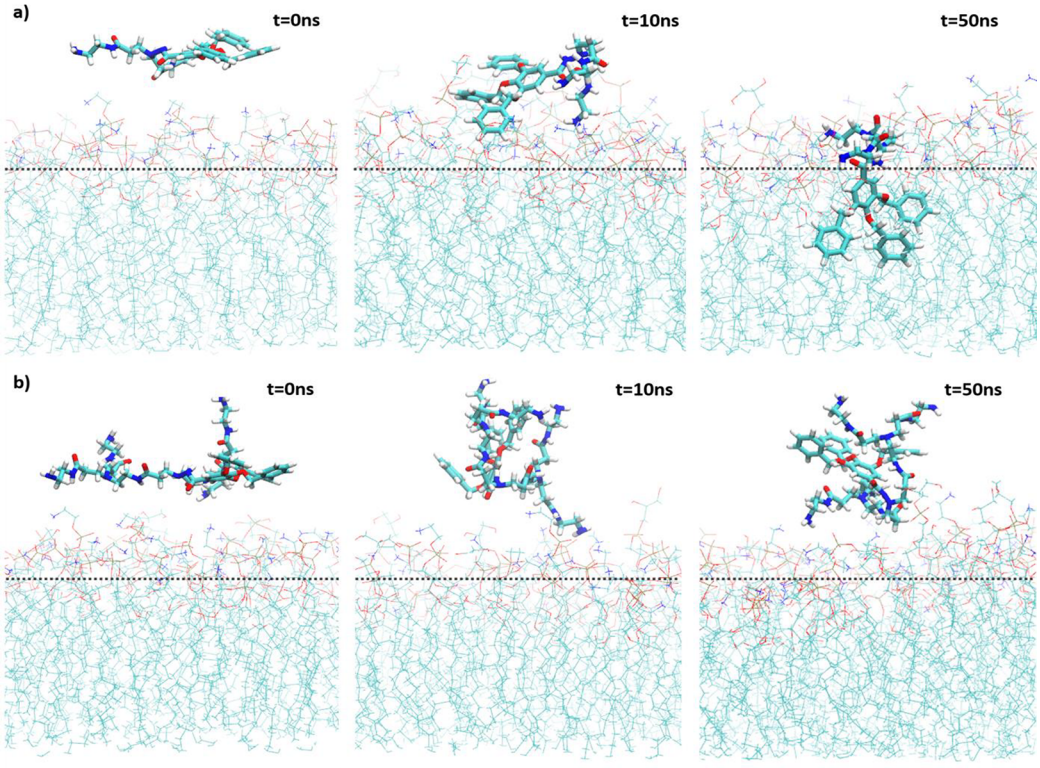

Figure 7. Time-dependent snapshots indicating the binding process of (a) **AD-1** and (b) **AD-3** dendrimers to the lipid bilayer. The dotted lines indicate the hydrophilic−hydrophobic interface at the lipid surface. Here, water molecules are not shown for clarity.

DOI: 10.1021/acsabm.9b00140
ACS Appl. Bio Mater. 2019, 2, 3212−3224

contribute to the antibacterial activity.[50,62] Also, MD simulations on cationic polymers and amphiphiles have shown that a facially amphiphilic conformation is more favorable for increased bacterial membrane lipid interactions.[64] Hence, MD simulations of **AD-1** and **AD-3** on bacterial membrane patches were performed.

Our 50 ns-long MD simulations revealed a favorable binding mode of **AD-1** within the initial 10 ns. However, **AD-3** was unable to bind to the membrane throughout the simulation time. The detailed binding process of dendrimers **AD-1** and **AD-3** on the bacterial membrane is explained in Figure 7, which shows the orientation of the dendrimers at different time steps of the simulation. First, **AD-1** was adsorbed on to the surface of bilayer due to the polar/electrostatic interactions between the branched amine terminal and the lipid head groups (Figure 7a, t = 10 ns). Second, **AD-1** was pulled into the bilayer because of the hydrophobic interactions between the poly(aryl ether) dendron moiety of **AD-1** and the lipid tails (Figure 7a, t = 50 ns). On the other hand, the branched amine terminal of **AD-3** showed interaction with the lipid head groups (Figure 7b, t = 10 ns) but did not result in specific binding to the bilayer due to the presence of larger hydrophilic extended arms in **AD-3** (Figure 7b, t = 50 ns). From the conformational orientation, it was observed that the hydrophilic flexible arm of **AD-3** dendrimer encloses the hydrophobic poly(aryl ether) dendron moiety in a cage-like structure, favoring its presence in water phase, and hence, penetration to the lipid bilayer was hindered. MD simulations of **AD-1** and **AD-3** on bacterial membrane patches are included as Movies S1 and S2 in the Supporting Information.

To track the position of the dendrimers, the time evolution of the z-component of distance between the center of mass (COM) of the dendrimer and the COM of the bilayer was plotted (Figure S18a). From Figure S18a, it was evident that **AD-1** showed random dynamics in water for ∼10 ns followed by its absorption into the bilayer, where it remained stable for the rest of the simulation time, indicating strong affinity. In contrast, **AD-3** oscillated randomly in water and did not show continuous interaction even at the end of 50 ns, indicating weak affinity. We further quantified the affinity of **AD-1** versus **AD-3** by computing the non-bonded interaction energy (Figure S18b). Upon absorption onto the bilayer surface (around 10 ns), the interaction energy of **AD-1** increased rapidly from 0 kJ/mol (no interaction) to ∼500 kJ/mol (strong interaction) (Figure S18b). However, **AD-3** showed a slight increase of ∼100 kJ/mol, indicating poor absorption to the surface. On the basis of these MD simulations, we propose that along with hydrophobicity, molecular conformations of the poly(aryl ether)-based dendrimers (**AD-1** and **AD-3**) also play a crucial role for potent antibacterial activity.

Cytotoxicity of the Amphiphilic Dendrimers. The major focus of the work is to study the intrinsic antibacterial activity of poly(aryl ether)-based amphiphilic dendrimers. *In vitro* antibacterial assays on Gram-positive and Gram-negative bacteria demonstrated that **AD-1** dendrimer was effective in killing bacteria at a lower concentration in comparison to the other dendrimers (Table 2). Moreover, structural tuning of optimal hydrophobicity with cationic surface charge showed pronounced antibacterial activity of **AD-1** compared to that of **AD-3** (Table 2, Figure 3). Earlier reports on the HLB balance of cationic amphiphiles for effective bacterial membrane disruption demonstrated that tuning the structural characteristics of an amphiphile also leads to reduced cytotoxicity.[26,58,62] Hence, to determine the cytotoxic effect of the amphiphilic dendrimers, an MTT assay was performed on NIH/3T3 mouse fibroblast cell lines for 24 and 48 h (Figure 8). The dendrimers were tested at

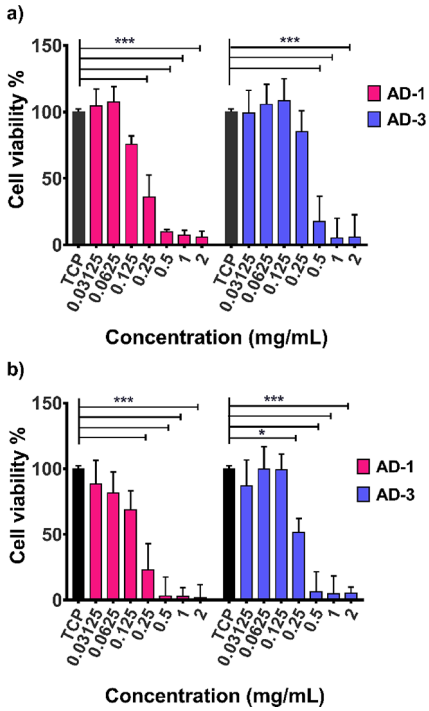

Figure 8. Cell viability of NIH/3T3 cells with various concentrations of **AD-1** and **AD-3** (0.0312−2 mg/mL) at (a) 24 and (b) 48 h. The percentage cell viability is calculated relative to the control well (tissue culture plate, TCP), n = 3, $^{**}p < 0.01$ and $^{***}p < 0.001$ vs control.

concentrations ranging from 0.0312−2 mg/mL. It was found that at higher concentration there is a decrease in cell viability on all four amphiphilic dendrimers (Figures 8a and b and Figure S19). NIH/3T3 fibroblast cells showed significant cytotoxicity only when they were exposed to **AD-1** at a concentration four times higher than the MIC (Figures 8a and b). The MBC of **AD-1** tested for both *E. coli* and *S. aureus* is found to be 0.125 mg/mL, indicating that only a double dosage of **AD-1** causes cytotoxicity. **AD-3** dendrimer, on the other hand, is cytotoxic at 0.5 mg/mL at 24 h (Figures 8a and b). However, the MBC of **AD-3** dendrimer is 2 mg/mL, making it cytotoxic at the concentrations found effective against bacteria. Similarly, dendrimers **AD-2** and **AD-4** were also tested for cytotoxicity, and the data are presented in the Supporting Information (Figure S19). Both **AD-2** and **AD-4** dendrimers show dose-dependent cytotoxicity at 24 and 48 h even below the MIC concentrations. However, there is no cytotoxicity observed for the **AD-1** dendrimer at its MIC concentration, making it an attractive biocompatible amphiphilic dendrimer with potent antibacterial activity. Also, we hope that fine-tuning of the structural characteristics of such amphiphiles would lead to the development of novel intrinsic antibacterial amphiphilic dendrimers with minimal cytotoxicity.

CONCLUSION

In summary, we demonstrated the antibacterial activity of poly(aryl ether)-based amphiphilic dendrimers by varying the surface charges and hydrophobicity. Amphiphilic dendrimer (**AD-1**) with an optimal surface charge to hydrophobicity ratio displayed effective membrane disruption in comparison to **AD-3**

DOI: 10.1021/acsabm.9b00140
ACS Appl. Bio Mater. 2019, 2, 3212−3224

dendrimer with higher surface cationic charges. Amphiphilic dendrimers **AD-2** and **AD-4** with optimal hydrophobicity but no cationic surface charges showed no antibacterial activity. The results establish a direct correlation between the cationic surface charge and hydrophobicity, indicating that (1) self-assembled **AD-1** dendrimers have electrostatic interaction with the lipid membrane followed by insertion into the membrane, leading to effective bacterial death; (2) **AD-3** amphiphilic dendrimers bind with strong electrostatic interactions to the bacterial membrane, but the flexible spacer arm does not provide sufficient insertion into the lipid membrane, eventually minimizing the antibacterial activity; and (3) **AD-1** dendrimer displays antibacterial activity similar to that of higher generation PAMAM dendrimers as a result of poly(aryl ether) mediated self-assembly. Further, MD simulations of **AD-1** and **AD-3** dendrimers on bacterial membrane patches elucidated the significance of conformational orientation of the dendrimers for potent bactericidal activity. The MD simulations showed that the hydrophobic dendron moiety was buried within the hydrophilic flexible arm of **AD-3**, leading to minimal bilayer interactions, while **AD-1** initially formed electrostatic interactions with the flexible arm, followed by hydrophobic interactions with the lipid membrane. Moreover, the amphiphilic dendrimers evaluated for their cytotoxicity also showed promising results. The amphiphilic dendrimer (**AD-3**) with high surface charge density displayed toxicity against NIH/3T3 at its MIC, while **AD-1** dendrimer with an optimal hydrophobicity showed no cytotoxicity even at four times the MIC values, unlike higher generation PAMAM-based dendrimers. Thus, a rational design approach in tuning the optimal balance between cationic surface groups and hydrophobicity of amphiphiles may lead to the development of antimicrobial amphiphilic dendrimers.

■ ASSOCIATED CONTENT

Supporting Information

The Supporting Information is available free of charge on the ACS Publications website at DOI: 10.1021/acsabm.9b00140.

^{1}H, ^{13}C, and HRMS data of amphiphilic dendrimers **AD-3** and **AD-4**, gelation table of the amphiphilic dendrimers, dendrimer aggregate stability in buffer and biological media, pK_a and protonated species at pH 7.4 of all four amphiphilic dendrimers, nonbonded energy interactions of **AD-1** and **AD-3** with lipid membrane, and cytotoxicity of **AD-2** and **AD-4** for 24 and 48 h (PDF)

MD simulation movie showing the trajectory of **AD-1** penetration to the bacterial lipid membrane (MPG)

MD simulation movie showing the evolution of **AD-3** on the surface of bacterial lipid membrane (MPG)

■ AUTHOR INFORMATION

Corresponding Authors

*E-mail: vigneshm@iitm.ac.in.
*E-mail: pre@iitm.ac.in.

ORCID

Sanjib Senapati: 0000-0002-6671-8299
Vignesh Muthuvijayan: 0000-0003-4921-9073
Edamana Prasad: 0000-0002-6643-1407

Author Contributions

The work was conceptualized by R.K., V.M., and E.P. Compound synthesis and characterization were performed by P.P. and R.B. Self-assembly and *in vitro* antibacterial and cytotoxicity studies were performed by R.K. with support from V.M. and E.P. MD simulations were performed by C.P. with support from S.S. All authors have seen and approved the final version of the submitted manuscript.

Notes

The authors declare no competing financial interest.

■ ACKNOWLEDGMENTS

The authors acknowledge funding from the Science & Engineering Research Board (SERB), Department of Science and Technology (DST), Government of India (Projects EMR/2016/003519 and ECR/2017/003064). We thank the Departments of Chemical Engineering and Chemistry, IIT Madras for SEM and computational facilities. Acknowledgments are due to Prof. Vani Janakiraman and Dr. Purva Bhatter for offering their cell culture expertise and facility. We thank Ms. Rubaiya and Prof. Mukesh Doble for the multiplate reader fluorimeter facility. P.P. thanks the University Grants Commission (UGC) for the fellowship, and R.K. thanks DST-INSPIRE for the fellowship and Interdisciplinary Program, IIT Madras.

■ REFERENCES

(1) Jones, K. E.; Patel, N. G.; Levy, M. A.; Storeygard, A.; Balk, D.; Gittleman, J. L.; Daszak, P. Global Trends in Emerging Infectious Diseases. *Nature* **2008**, *451* (7181), 990−993.

(2) Davies, J.; Davies, D. Origins and Evolution of Antibiotic Resistance. *Microbiol. Mol. Biol. Rev.* **2010**, *74* (3), 417−433.

(3) Andersson, D. I.; Hughes, D. Antibiotic Resistance and Its Cost: Is It Possible to Reverse Resistance? *Nat. Rev. Microbiol.* **2010**, *8* (4), 260−271.

(4) Simpkin, V. L.; Renwick, M. J.; Kelly, R.; Mossialos, E. Incentivising Innovation in Antibiotic Drug Discovery and Development: Progress, Challenges and next Steps. *J. Antibiot.* **2017**, *70* (12), 1087−1096.

(5) Sun, H.; Hong, Y.; Xi, Y.; Zou, Y.; Gao, J.; Du, J. Synthesis, Self-Assembly, and Biomedical Applications of Antimicrobial Peptide−Polymer Conjugates. *Biomacromolecules* **2018**, *19* (6), 1701−1720.

(6) Lam, S. J.; O'Brien-Simpson, N. M.; Pantarat, N.; Sulistio, A.; Wong, E. H. H.; Chen, Y.-Y.; Lenzo, J. C.; Holden, J. A.; Blencowe, A.; Reynolds, E. C.; et al. Combating Multidrug-Resistant Gram-Negative Bacteria with Structurally Nanoengineered Antimicrobial Peptide Polymers. *Nat. Microbiol.* **2016**, *1* (11), 16162.

(7) Walsh, C. Molecular Mechanisms That Confer Antibacterial Drug Resistance. *Nature* **2000**, *406* (6797), 775−781.

(8) Kohanski, M. A.; Dwyer, D. J.; Collins, J. J. How Antibiotics Kill Bacteria: From Targets to Networks. *Nat. Rev. Microbiol.* **2010**, *8* (6), 423−435.

(9) Hurdle, J. G.; O'Neill, A. J.; Chopra, I.; Lee, R. E. Targeting Bacterial Membrane Function: An Underexploited Mechanism for Treating Persistent Infections. *Nat. Rev. Microbiol.* **2011**, *9* (1), 62−75.

(10) Nikaido, H. Prevention of Drug Access to Bacterial Targets: Permeability Barriers and Active Efflux. *Science (Washington, DC, U. S.)* **1994**, *264* (5157), 382−388.

(11) Herzog, I. M.; Fridman, M. Design and Synthesis of Membrane-Targeting Antibiotics: From Peptides- to Aminosugar-Based Antimicrobial Cationic Amphiphiles. *MedChemComm* **2014**, *5* (8), 1014−1026.

(12) Brogden, K. A. Antimicrobial Peptides: Pore Formers or Metabolic Inhibitors in Bacteria? *Nat. Rev. Microbiol.* **2005**, *3* (3), 238−250.

(13) Shai, Y. Mode of Action of Membrane Active Antimicrobial Peptides. *Biopolymers* **2002**, *66* (4), 236−248.

(14) Marr, A.; Gooderham, W.; Hancock, R. Antibacterial Peptides for Therapeutic Use: Obstacles and Realistic Outlook. *Curr. Opin. Pharmacol.* **2006**, *6* (5), 468−472.

DOI: 10.1021/acsabm.9b00140
ACS Appl. Bio Mater. 2019, 2, 3212−3224

(15) Findlay, B.; Zhanel, G. G.; Schweizer, F. Cationic Amphiphiles, a New Generation of Antimicrobials Inspired by the Natural Antimicrobial Peptide Scaffold. *Antimicrob. Agents Chemother.* **2010**, *54* (10), 4049−4058.
(16) Ghosh, C.; Manjunath, G. B.; Akkapeddi, P.; Yarlagadda, V.; Hoque, J.; Uppu, D. S. S. M.; Konai, M. M.; Haldar, J. Small Molecular Antibacterial Peptoid Mimics: The Simpler the Better! *J. Med. Chem.* **2014**, *57* (4), 1428−1436.
(17) Goswami, S.; Adhikari, M. D.; Kar, C.; Thiyagarajan, D.; Das, G.; Ramesh, A. Synthetic Amphiphiles as Therapeutic Antibacterials: Lessons on Bactericidal Efficacy and Cytotoxicity and Potential Application as an Adjuvant in Antimicrobial Chemotherapy. *J. Mater. Chem. B* **2013**, *1* (20), 2612−2623.
(18) Faig, A.; Arthur, T. D.; Fitzgerald, P. O.; Chikindas, M.; Mintzer, E.; Uhrich, K. E. Biscationic Tartaric Acid-Based Amphiphiles: Charge Location Impacts Antimicrobial Activity. *Langmuir* **2015**, *31* (43), 11875−11885.
(19) Zhou, C.; Wang, F.; Chen, H.; Li, M.; Qiao, F.; Liu, Z.; Hou, Y.; Wu, C.; Fan, Y.; Liu, L.; et al. Selective Antimicrobial Activities and Action Mechanism of Micelles Self-Assembled by Cationic Oligomeric Surfactants. *ACS Appl. Mater. Interfaces* **2016**, *8* (6), 4242−4249.
(20) Canalle, L. A.; Löwik, D. W. P. M.; van Hest, J. C. M. Polypeptide−Polymer Bioconjugates. *Chem. Soc. Rev.* **2010**, *39* (1), 329−353.
(21) Song, A.; Walker, S. G.; Parker, K. A.; Sampson, N. S. Antibacterial Studies of Cationic Polymers with Alternating, Random, and Uniform Backbones. *ACS Chem. Biol.* **2011**, *6* (6), 590−599.
(22) Shen, W.; He, P.; Xiao, C.; Chen, X. From Antimicrobial Peptides to Antimicrobial Poly(α-Amino Acid)S. *Adv. Healthcare Mater.* **2018**, *7* (20), 1800354.
(23) Hancock, R. E. W.; Scott, M. G. The Role of Antimicrobial Peptides in Animal Defenses. *Proc. Natl. Acad. Sci. U. S. A.* **2000**, *97* (16), 8856−8861.
(24) Stupp, S. I. Self-Assembly and Biomaterials. *Nano Lett.* **2010**, *10* (12), 4783−4786.
(25) Zhang, S. Fabrication of Novel Biomaterials through Molecular Self-Assembly. *Nat. Biotechnol.* **2003**, *21* (10), 1171−1178.
(26) Qi, R.; Zhang, P.; Liu, J.; Zhou, L.; Zhou, C.; Zhang, N.; Han, Y.; Wang, S.; Wang, Y. Peptide Amphiphiles with Distinct Supramolecular Nanostructures for Controlled Antibacterial Activities. *ACS Appl. Bio Mater.* **2018**, *1* (1), 21−26.
(27) Zhou, C.; Wang, H.; Bai, H.; Zhang, P.; Liu, L.; Wang, S.; Wang, Y. Tuning Antibacterial Activity of Cyclodextrin-Attached Cationic Ammonium Surfactants by a Supramolecular Approach. *ACS Appl. Mater. Interfaces* **2017**, *9* (37), 31657−31666.
(28) Schnaider, L.; Brahmachari, S.; Schmidt, N. W.; Mensa, B.; Shaham-Niv, S.; Bychenko, D.; Adler-Abramovich, L.; Shimon, L. J. W.; Kolusheva, S.; DeGrado, W. F.; et al. Self-Assembling Dipeptide Antibacterial Nanostructures with Membrane Disrupting Activity. *Nat. Commun.* **2017**, *8* (1), 1365.
(29) Fukushima, K.; Tan, J. P. K.; Korevaar, P. A.; Yang, Y. Y.; Pitera, J.; Nelson, A.; Maune, H.; Coady, D. J.; Frommer, J. E.; Engler, A. C.; et al. Broad-Spectrum Antimicrobial Supramolecular Assemblies with Distinctive Size and Shape. *ACS Nano* **2012**, *6* (10), 9191−9199.
(30) Hoque, J.; Konai, M. M.; Samaddar, S.; Gonuguntala, S.; Manjunath, G. B.; Ghosh, C.; Haldar, J. Selective and Broad Spectrum Amphiphilic Small Molecules to Combat Bacterial Resistance and Eradicate Biofilms. *Chem. Commun.* **2015**, *51* (71), 13670−13673.
(31) Bai, J.; Chen, C.; Wang, J.; Zhang, Y.; Cox, H.; Zhang, J.; Wang, Y.; Penny, J.; Waigh, T.; Lu, J. R.; et al. Enzymatic Regulation of Self-Assembling Peptide A9K2 Nanostructures and Hydrogelation with Highly Selective Antibacterial Activities. *ACS Appl. Mater. Interfaces* **2016**, *8* (24), 15093−15102.
(32) Yuan, W.; Wei, J.; Lu, H.; Fan, L.; Du, J. Water-Dispersible and Biodegradable Polymer Micelles with Good Antibacterial Efficacy. *Chem. Commun.* **2012**, *48* (54), 6857.
(33) Qiao, Y.; Yang, C.; Coady, D. J.; Ong, Z. Y.; Hedrick, J. L.; Yang, Y.-Y. Highly Dynamic Biodegradable Micelles Capable of Lysing Gram-Positive and Gram-Negative Bacterial Membrane. *Biomaterials* **2012**, *33* (4), 1146−1153.
(34) Sowińska, M.; Laskowska, A.; Guśpiel, A.; Solecka, J.; Bochynska-Czyz, M.; Lipkowski, A. W.; Trzeciak, K.; Urbanczyk-Lipkowska, Z. Bioinspired Amphiphilic Peptide Dendrimers as Specific and Effective Compounds against Drug Resistant Clinical Isolates of E Coli. *Bioconjugate Chem.* **2018**, *29* (11), 3571−3585.
(35) Wang, B.; Navath, R. S.; Menjoge, A. R.; Balakrishnan, B.; Bellair, R.; Dai, H.; Romero, R.; Kannan, S.; Kannan, R. M. Inhibition of Bacterial Growth and Intramniotic Infection in a Guinea Pig Model of Chorioamnionitis Using PAMAM Dendrimers. *Int. J. Pharm.* **2010**, *395* (1−2), 298−308.
(36) Felczak, A.; Wrońska, N.; Janaszewska, A.; Klajnert, B.; Bryszewska, M.; Appelhans, D.; Voit, B.; Rózalska, S.; Lisowska, K. Antimicrobial Activity of Poly(Propylene Imine) Dendrimers. *New J. Chem.* **2012**, *36* (11), 2215−2222.
(37) Strydom, S. J.; Rose, W. E.; Otto, D. P.; Liebenberg, W.; de Villiers, M. M. Poly(Amidoamine) Dendrimer-Mediated Synthesis and Stabilization of Silver Sulfonamide Nanoparticles with Increased Antibacterial Activity. *Nanomedicine* **2013**, *9* (1), 85−93.
(38) Gholami, M.; Mohammadi, R.; Arzanlou, M.; Akbari Dourbash, F.; Kouhsari, E.; Majidi, G.; Mohseni, S. M.; Nazari, S. In Vitro Antibacterial Activity of Poly (Amidoamine)-G7 Dendrimer. *BMC Infect. Dis.* **2017**, *17* (1), 395.
(39) Feng, Y.; Liu, Z. T.; Liu, J.; He, Y. M.; Zheng, Q. Y.; Fan, Q. H. Peripherally Dimethyl Isophthalate-Functionalized Poly(Benzyl Ether) Dendrons: A New Kind of Unprecedented Highly Efficient Organogelators. *J. Am. Chem. Soc.* **2009**, *131* (23), 7950−7951.
(40) Kannan, R.; Muthuvijayan, V.; Prasad, E. In Vitro Study of a Glucose Attached Poly(Aryl Ether) Dendron Based Gel as a Drug Carrier for a Local Anaesthetic. *New J. Chem.* **2017**, *41* (15), 7453−7462.
(41) Satapathy, S.; Prabakaran, P.; Prasad, E. Augmenting Photo-induced Charge Transport in a Single-Component Gel System: Controlled In Situ Gel-Crystal Transformation at Room Temperature. *Chem. - Eur. J.* **2018**, *24* (23), 6217−6230.
(42) Malakar, P.; Prasad, E. Self-Assembly and Gelation of Poly(Aryl Ether) Dendrons Containing Hydrazide Units: Factors Controlling the Formation of Helical Structures. *Chem. - Eur. J.* **2015**, *21* (13), 5093−5100.
(43) Rajamalli, P.; Prasad, E. Tunable Morphology and Mesophase Formation by Naphthalene-Containing Poly(Aryl Ether) Dendron-Based Low-Molecular-Weight Fluorescent Gels. *Langmuir* **2013**, *29* (5), 1609−1617.
(44) Prabakaran, P.; Prasad, E. Janus Dendrimer from Poly(Aryl Ether) Linked PAMAM for Supergelation and Guest Release. *ChemistrySelect* **2016**, *1* (17), 5561−5568.
(45) Tetko, I. V.; Gasteiger, J.; Todeschini, R.; Mauri, A.; Livingstone, D.; Ertl, P.; Palyulin, V. A.; Radchenko, E. V.; Zefirov, N. S.; Makarenko, A. S.; et al. Virtual Computational Chemistry Laboratory − Design and Description. *J. Comput.-Aided Mol. Des.* **2005**, *19* (6), 453−463.
(46) Szendi, B.; Lakatos, I. Determination of Minimum Inhibitory Concentrations (MICs) of Antibacterial Agents by Broth Dilution. *Clin. Microbiol. Infect.* **2003**, *9* (8), 1−7.
(47) Sträuber, H.; Müller, S. Viability States of Bacteria-Specific Mechanisms of Selected Probes. *Cytometry, Part A* **2010**, *77A* (7), 623−634.
(48) Cabrini, G.; Verkman, A. S. Potential-Sensitive Response Mechanism of $DiSC_3(5)$ in Biological Membranes. *J. Membr. Biol.* **1986**, *92* (2), 171−182.
(49) Jo, S.; Kim, T.; Iyer, V. G.; Im, W. CHARMM-GUI: A Web-Based Graphical User Interface for CHARMM. *J. Comput. Chem.* **2008**, *29* (11), 1859−1865.
(50) Zhang, Y.; Algburi, A.; Wang, N.; Kholodovych, V.; Oh, D. O.; Chikindas, M.; Uhrich, K. E. Self-Assembled Cationic Amphiphiles as Antimicrobial Peptides Mimics: Role of Hydrophobicity, Linkage Type, and Assembly State. *Nanomedicine* **2017**, *13* (2), 343−352.

DOI: 10.1021/acsabm.9b00140
ACS Appl. Bio Mater. 2019, 2, 3212−3224

(51) Frisch, M. J.; Trucks, G. W.; Schlegel, H. B.; Scuseria, G. E.; Robb, M. A.; Cheeseman, J. R.; Scalmani, G.; Barone, V.; Mennucci, B.; Petersson, G. A.; Nakatsuji, H.; Caricato, M.; Li, X.; Hratchian, H. P.; Izmaylov, A. F.; Bloino, J.; Zheng, G.; Sonnenberg, J. L.; Hada, M.; Ehara, M.; Toyota, K.; Fukuda, R.; Hasegawa, J.; Ishida, M.; Nakajima, T.; Honda, Y.; Kitao, O.; Nakai, H.; Vreven, T.; Montgomery, J. A., Jr.; Peralta, J. E.; Ogliaro, F.; Bearpark, M.; Heyd, J. J.; Brothers, E.; Kudin, K. N.; Staroverov, V. N.; Kobayashi, R.; Normand, J.; Raghavachari, K.; Rendell, A.; Burant, J. C.; Iyengar, S. S.; Tomasi, J.; Cossi, M.; Rega, N.; Millam, J. M.; Klene, M.; Knox, J. E.; Cross, J. B.; Bakken, V.; Adamo, C.; Jaramillo, J.; Gomperts, R.; Stratmann, R. E.; Yazyev, O.; Austin, A. J.; Cammi, R.; Pomelli, C.; Ochterski, J. W.; Martin, R. L.; Morokuma, K.; Zakrzewski, V. G.; Voth, G. A.; Salvador, P.; Dannenberg, J. J.; Dapprich, S.; Daniels, A. D.; Farkas, O.; Foresman, J. B.; Ortiz, J. V.; Cioslowski, J.; Fox, D. J. *Gaussian 09*, revision A.2; Gaussian, Inc.: Wallingford, CT, 2009.

(52) Case, D. A.; Babin, V.; Berryman, J. T.; Betz, R. M.; Cai, Q.; Cerutti, D. S.; Cheatham, T. E., III; Darden, T. A.; Duke, R. E.; Gohlke, H.; Goetz, A. W.; Gusarov, S.; Homeyer, N.; Janowski, P.; Kaus, J.; Kolossváry, I.; Lee, T. S.; LeGrand, S.; Luchko, T.; Luo, R.; Madej, B.; Merz, K. M.; Paesani, F.; Roe, D. R.; Roitberg, A.; Sagui, C.; Salomon-Ferrer, R.; Seabra, G.; Simmerling, C. L.; Smith, W.; Swails, J.; Walker, R. C.; Wang, J.; Wolf, R. M.; Wu, X.; Kollman, P. A. *AMBER 14*; University of California: San Francis, 2014.

(53) Ferrari, M.; Fornasiero, M. C.; Isetta, A. M. MTT Colorimetric Assay for Testing Macrophage Cytotoxic Activity in Vitro. *J. Immunol. Methods* **1990**, *131* (2), 165−172.

(54) Xue, X.; Chen, X.; Mao, X.; Hou, Z.; Zhou, Y.; Bai, H.; Meng, J.; Da, F.; Sang, G.; Wang, Y.; et al. Amino-Terminated Generation 2 Poly(Amidoamine) Dendrimer as a Potential Broad-Spectrum, Non-resistance-Inducing Antibacterial Agent. *AAPS J.* **2013**, *15* (1), 132−142.

(55) Lopez, A. I.; Reins, R. Y.; McDermott, A. M.; Trautner, B. W.; Cai, C. Antibacterial Activity and Cytotoxicity of PEGylated Poly-(Amidoamine) Dendrimers. *Mol. BioSyst.* **2009**, *5* (10), 1148−1156.

(56) Malekkhaiat Häffner, S.; Malmsten, M. Influence of Self-Assembly on the Performance of Antimicrobial Peptides. *Curr. Opin. Colloid Interface Sci.* **2018**, *38*, 56−79.

(57) Ebejer, J. P.; Charlton, M. H.; Finn, P. W. Are the Physicochemical Properties of Antibacterial Compounds Really Different from Other Drugs? *J. Cheminf.* **2016**, *8* (1), 1−9.

(58) Yamamura, H.; Miyagawa, A.; Sugiyama, H.; Murata, K.; Mabuti, T.; Mitsuhashi, R.; Hagiwara, T.; Nonaka, M.; Tanimoto, K.; Tomita, H. Rule of Hydrophobicity/Hydrophilicity Balance in Membrane-Disrupting Antimicrobial Activity of Polyalkylamino Cyclodextrins Synthesized via Click Chemistry. *ChemistrySelect* **2016**, *1* (3), 469−472.

(59) Hoque, J.; Konai, M. M.; Sequeira, S. S.; Samaddar, S.; Haldar, J. Antibacterial and Antibiofilm Activity of Cationic Small Molecules with Spatial Positioning of Hydrophobicity: An in Vitro and in Vivo Evaluation. *J. Med. Chem.* **2016**, *59* (23), 10750−10762.

(60) Alves, C. S.; Melo, M. N.; Franquelim, H. G.; Ferre, R.; Planas, M.; Feliu, L.; Bardají, E.; Kowalczyk, W.; Andreu, D.; Santos, N. C.; et al. Escherichia Coli Cell Surface Perturbation and Disruption Induced by Antimicrobial Peptides BP100 and PepR. *J. Biol. Chem.* **2010**, *285* (36), 27536−27544.

(61) Goswami, S.; Thiyagarajan, D.; Das, G.; Ramesh, A. Biocompatible Nanocarrier Fortified with a Dipyridinium-Based Amphiphile for Eradication of Biofilm. *ACS Appl. Mater. Interfaces* **2014**, *6* (18), 16384−16394.

(62) Konai, M. M.; Samaddar, S.; Bocchinfuso, G.; Santucci, V.; Stella, L.; Haldar, J. Selectively Targeting Bacteria by Tuning the Molecular Design of Membrane-Active Peptidomimetic Amphiphiles. *Chem. Commun.* **2018**, *54* (39), 4943−4946.

(63) Chen, C.; Pan, F.; Zhang, S.; Hu, J.; Cao, M.; Wang, J.; Xu, H.; Zhao, X.; Lu, J. R. Antibacterial Activities of Short Designer Peptides: A Link between Propensity for Nanostructuring and Capacity for Membrane Destabilization. *Biomacromolecules* **2010**, *11* (2), 402−411.

(64) Palermo, E. F.; Vemparala, S.; Kuroda, K. Cationic Spacer Arm Design Strategy for Control of Antimicrobial Activity and Conformation of Amphiphilic Methacrylate Random Copolymers. *Biomacromolecules* **2012**, *13* (5), 1632−1641.

DOI: 10.1021/acsabm.9b00140
ACS Appl. Bio Mater. 2019, 2, 3212−3224